Chapter 8
Advanced 3D Imaging and Transcatheter Valve Repair/Implantation

Derek Phan, Santanu Biswas, and Sameer Gafoor

Abbreviations

2D	Two-dimensional
3D	Three-dimensional
4D	Four-dimensional
AV	Atrioventricular
CS	Coronary sinus
CT	Computed tomography
ECG	Electrocardiogram
IVC	Inferior vena cava
LCX	Left circumflex artery
LVOT	Left ventricular outflow tract
MA	Mitral annulus
MRI	Magnetic resonance imaging
RA	Right atrium
RCA	Right coronary artery
RV	Right ventricle
SVC	Superior vena cava
TAVI	Transcatheter aortic valve implantation
TEE	Transesophageal echocardiography
TMVr	Transcatheter mitral valve repair

D. Phan · S. Biswas
Swedish Heart and Vascular, Seattle, WA, USA

S. Gafoor (✉)
Swedish Heart and Vascular, Seattle, WA, USA

Cardiovascular Center Frankfurt, Frankfurt, Germany

P. A. Iaizzo et al. (eds.), *Heart Valves*, https://doi.org/10.1007/978-3-031-25541-0_8

TMVR	Transcatheter mitral valve replacement
TV	Tricuspid valve

8.1 Introduction

Valvular heart disease is a major cause of morbidity and mortality in developing and industrialized countries. While rheumatic and infectious causes are more common in developing countries, degenerative valvular disease is the predominant etiology in the aging population of the industrialized world. For patients with advanced, symptomatic disease, surgical open-heart valve replacement or repair remains the standard treatment with excellent short- and long-term outcomes. However, there is a significant percentage of typically older patients that are not considered surgical candidates. For example, in Europe and the United States surveys, about 30% of patients with severe symptomatic aortic stenosis are not considered surgical candidates secondary to advanced age and comorbidities [1]. Because these patients have a poor outcome with medical management [2–5], less-invasive transcatheter approaches for valve repair/implantation appear promising for subgroups of these high-risk patients.

Transcatheter aortic valve implantation (TAVI) for symptomatic patients with severe aortic stenosis utilizes stent systems, in which a bioprosthetic valve is mounted. The procedure can be performed using a transfemoral, transcaval, transcarotid, transaxillary, transaortic, or transapical approach [6–11]. The stent/valve systems are anchored at the annulus and extend into the root or proximal ascending aorta. Since the initial successful human implantation in 2002, different generations of balloon-expandable or self-expandable valve prostheses have been implanted in several thousand patients with severe symptomatic aortic stenosis. The results in experienced centers are good, with high implantation success rate, significant hemodynamic and clinical improvements, and improved survival rates [11–13]. TAVI was associated with improved outcomes compared to medical therapy, and comparable outcomes to open-heart surgery [14]. See chapter on TAVI devices for more information.

There are several percutaneous approaches for the treatment of mitral regurgitation, including both transcatheter mitral valve repair (TMVr) and replacement (TMVR). The most common percutaneous mitral valve repair procedure is derived from the Alfieri edge-to-edge repair, which consists of suturing the free edges of the anterior and posterior mitral leaflets [15, 16]. The transcatheter procedure deploys a clip to join the free edges of the opposing leaflets, thus creating a double-orifice valve [17–20]. Alternative percutaneous procedures include coronary sinus (CS) annuloplasty with placement of devices in the CS. The goal is to displace the posterior portion of mitral annulus (MA), in order to improve the coaptation of the leaflets [21–24]. One study [24] showed the feasibility of percutaneous reduction in functional mitral regurgitation with a CS-based mitral annuloplasty device in patients with heart failure and was associated with an improvement in quality of life and exercise tolerance. For prosthetic mitral valve paravalvular regurgitation, percutaneous device closure has been successful. Several TMVR devices are currently under clinical investigation, and mitral valve-in-valve implantation with an aortic transcatheter valve has been performed with much success. See chapter on transcatheter mitral valve repair and replacement devices for more information.

Transcatheter pulmonic valve replacement has also been established in patients with dysfunctional right ventricular outflow tract conduits and pulmonary regurgitation [25, 26]. More information on transcatheter pulmonic valve replacement is in future chapters.

Recent studies also describe transcatheter tricuspid valve implantation [27] and valve-in-valve implantation [28, 29]. Transcatheter tricuspid valve repair or replacement is a rapidly advancing field. Several therapies are currently under investigation, including suture or ring annuloplasty devices, coaptation devices (edge-to-edge repair), direct valve replacement, and caval (superior or inferior vena cava) implantation devices. Tricuspid valve edge-to-edge repair is currently the most commonly used method and heavily relies on two-dimensional (2D) and three-dimensional (3D) transesophageal echocardiography for technical success.

As described in more detail in other chapters of the book, transcatheter valvular procedures are becoming an alternative to open surgical approaches in selected patient populations. Low frequency of procedural-related complications and good long-term outcomes depend on careful selection of potential candidates, with an important role for imaging [30].

8.2 Imaging in the Context of Transcatheter Valve Procedures

Due to the lack of direct visualization of the operative field during transcatheter procedures, imaging for preoperative planning and intraoperative guidance is an integral component of transcatheter procedures [31, 32].

Standard 2D imaging is performed with conventional X-ray angiography and echocardiography before and during the procedure. Since angiography and echocardiography create 2D projections or acquire 2D planes, understanding of 3D relationships requires viewing and mentally reconstructing the object from multiple different projections or planes. In contrast, 3D imaging provides 3D visualization and is increasingly used for pre- and intraoperative visualization [33–37]. Three-dimensional imaging modalities include 3D echocardiography, computed tomography (CT), C-arm CT, and magnetic resonance imaging (MRI).

Three-dimensional echocardiography [38, 39] is used for real-time procedural image guidance during catheter-based therapies. Three-dimensional transthoracic and transesophageal echocardiography (TEE) is performed with rectangular (or matrix) array transducers, which acquire a 3D pyramidal data volume [39–42]. With a full-volume acquisition, commonly acquired over several cardiac cycles, a full 3D data set with high temporal and spatial resolution can be obtained. Similar to CT, offline reconstruction generates multiple 2D cut planes that can be applied to display structures of interest from different perspectives. This approach allows reconstruction of images orthogonal to the vessel's centerline for measurement, e.g., of the aortic annulus. Alternatively, 3D data acquisition can be real time, with a slightly lower temporal resolution compared to full 3D data sets obtained over several cardiac cycles. Real-time 3D echocardiography is especially useful in the guidance of mitral valve procedures, as it provides the unique enface viewing perspective of the mitral valve from the left atrium (often termed the "surgeon's view"). Further, the 3D matrix probe also allows the simultaneous real-time display of two adjustable image planes at high temporal and spatial quality, in both 2D and color Doppler modes. This is especially important for color Doppler imaging where low temporal resolution often significantly limits the use of true 3D techniques such as real-time and full-volume acquisitions. Biplane imaging is particularly useful in assessing mitral, aortic, and tricuspid valve pathologies where high spatial and temporal resolutions similar to 2D echocardiography are often needed, but simultaneous imaging of two planes helps to assess the 3D structure. Initial experience with 3D TEE demonstrates its value in the clinical evaluation of structural heart disease, intraoperative assessment, and guidance of interventional procedures [43–49].

C-arm CT describes the use of CT-like acquisition and reconstruction techniques to obtain 3D data with C-arm-based X-ray angiography systems. The C-arm is rotated over a wide arc (>180°) around the patient typically during continuous contrast injection, acquiring multiple views of the cardiovascular structure in order to reconstruct a 3D image [50, 51]. For electrocardiogram (ECG)-referenced cardiac imaging, alternating forward and backward rotations are triggered by the ECG signal to acquire projections covering the entire acquisition range at a similar cardiac phase. C-arm CT has shown potential for use during various cardiovascular interventional procedures including coronary angiography and percutaneous coronary interventions [52, 53], pulmonary vein isolation [54], and endovascular stent repair of aortic disease [55].

The use of CT for cardiovascular indications has become possible due to improvements of spatial and temporal resolution and an increased number of detector systems [56–58]. Using dual-tube technology, temporal resolution of 75 ms can be achieved with a spatial resolution of about 0.5 mm and slice thickness of about 0.5–0.75 mm. With 320-slice systems, 16 cm can be covered in one rotation. These isotropic data sets allow oblique reconstruction without degradation of spatial resolution. Most imaging experience in the context of transcatheter valve procedures is based on retrospectively ECG-gated helical acquisitions (typically with use of tube current modulation, but a wide dose modulation window). The ECG-synchronized image acquisition throughout the cardiac cycle allows reconstruction at any point throughout the R-R interval, and cine display of multiple phases throughout the cardiac cycle permits dynamic display of cardiac and valvular motion, as well as reconstruction at specific positions in the R-R interval. For example, visualization of a plane at the tip of the leaflets at different times during the cardiac cycle allows determination of the maximal opening of the aortic valve during the cardiac cycle by planimetry (typically mid-late systole). However, the temporal resolution of CT is lower than that of echocardiography and MRI.

These CT protocols are usually associated with increased radiation exposure [59–61]. Careful individual planning of the imaging protocol and consideration of potential alternative imaging modalities are important to control radiation exposure [62]. Strategies associated with lower doses for cardiovascular CT imaging include tube current modulation with retrospective ECG-gated helical imaging, prospectively ECG-triggered imaging techniques, and use of low X-ray tube voltage (e.g., 100 kVp) [63–67]. If four-dimensional (4D) imaging is not necessary, prospective ECG-triggered axial acquisitions focused on a specific phase in the cardiac cycle should be preferred in patients with stable heart rate, because of the significantly lower radiation exposure. Most protocols are performed after intravenous contrast administration. If contrast administration is not feasible, non-contrast images can be useful to visualize calcification of the valve and/or aortic root and remaining segments of the vasculature, although precise measurements may be difficult.

Interventional cardiovascular MR techniques have been developed to guide transcatheter procedures [68–72]. The advantage of these approaches is that they provide good soft tissue visualization and functional assessment, including blood flow without radiation exposure. However, they add significant complexity to the procedure and require special compatible instruments and considerable capital investment [73]. An important concept is the development of MR road maps, which are combined with live X-ray fluoroscopy using a conventional clinical environment and conventional catheter equipment (Fig. 8.1). Such data provide additional anatomic landmarks and functional information to guide procedures [74, 75]. Magnetic resonance might aid in positioning nonsurgical replacement of heart valves, relative to vital structures such as coronary artery ostia [69]. A limitation of MRI in the context of TAVI is the signal void caused by calcium and metal, which precludes precise assessment of densely calcified valves and after stent-valve placement.

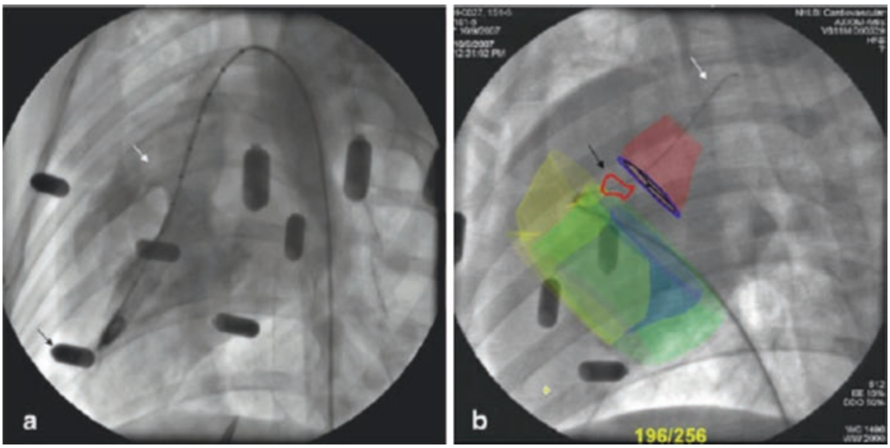

Fig. 8.1 Interventional MRI and angiographic fusion. Interventional applications of MRI allow real-time fusion of angiographic and MRI images in hybrid MRI/angiosuites for direct procedural guidance. (Image courtesy of Dr. Lederman; adapted with permission from Ratnayaka et al. [74])

8.2.1 Transcatheter Aortic Valve Implantation

8.2.1.1 Anatomy

Aortic root anatomy, including the aortic valve and coronary artery ostia, is complex [76–78]. The geometry and relationship of the aortic root structures change throughout the cardiac cycle [79–82]. Implantation of a stent/valve is incompletely understood, including the consequences of these structures and their relationships.

The aortic annulus describes the interface between the left ventricular outflow tract and the aortic root at the commissures of the aortic valve leaflets (Fig. 8.2). The three commissures extend upward into the aortic root similar to the shape of a crown or the struts of a bioprosthetic valve. The "annular" level at the lowest point of the valve hinge point ("inferior virtual basal ring") defines the level where valve prostheses are sutured or secured. During valve surgery, the annulus is fitted to the valve. On the other hand, when the transcatheter valve is deployed, the stent/valve must adjust to the "aortic root." Therefore, in addition to size and shape, the composition and material properties of the surrounding structures have important implications for the interaction between device and root. Approximately two-third are in contact

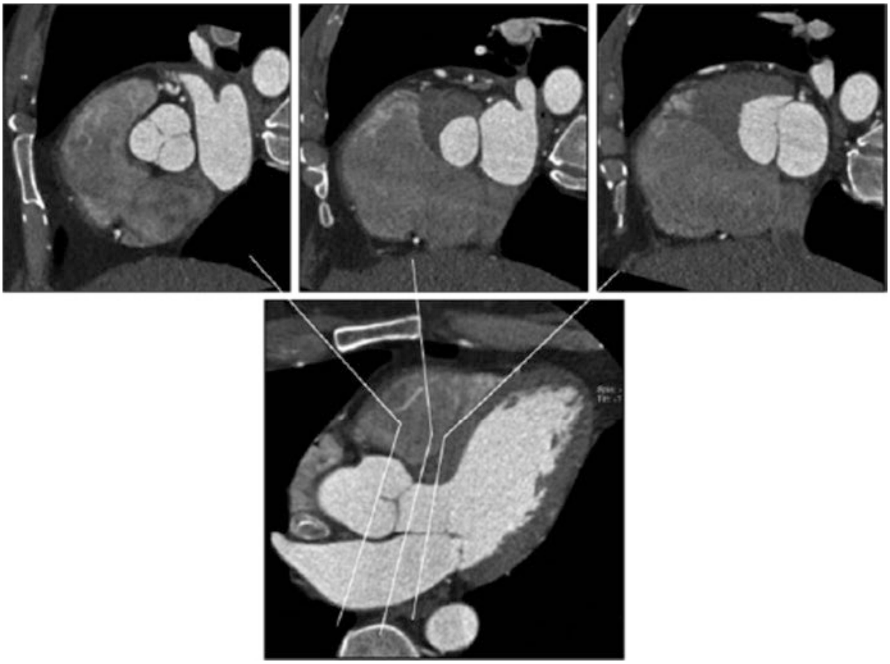

Fig. 8.2 Relationship between aortic valve, left ventricular outflow tract (LVOT), and anterior mitral leaflet. The upper panels show (*left* to *right*) cross sections through aortic valve, LVOT, and anterior mitral leaflet. The close relationship between these structures is demonstrated

with ventricular myocardium, and the remaining one-third are composed of the aortic leaflet of the mitral valve [31].

The three individual cusps of the aortic valve are attached to the aortic wall along the commissures in a crescentic fashion (Fig. 8.3). Behind the cusps are the outward bulging sinuses of Valsalva, with the origins of the coronary arteries at the superior aspect of the left and right aortic sinuses. There is a wide variation in distance between the leaflet tips and the coronary ostia, and in about 50% of patients, the length of the left coronary leaflet exceeds the distance between the annulus and the ostium of the left coronary artery. This has important implications during pre-procedural planning for TAVI, especially when evaluating risk of coronary obstruction with valve implantation.

The sinotubular junction describes the margin between the aortic root and tubular ascending aorta and has an important role in maintaining valve competence (Fig. 8.4) [83]. During the TAVI procedures, the sinotubular junction provides support for the deployment balloon; depending on valve design (short vs. long), the sinotubular junction and proximal ascending aorta are important for proper implantation (distal anchor zone). Please see Chap. 2 for more information on the anatomy of the semilunar valves.

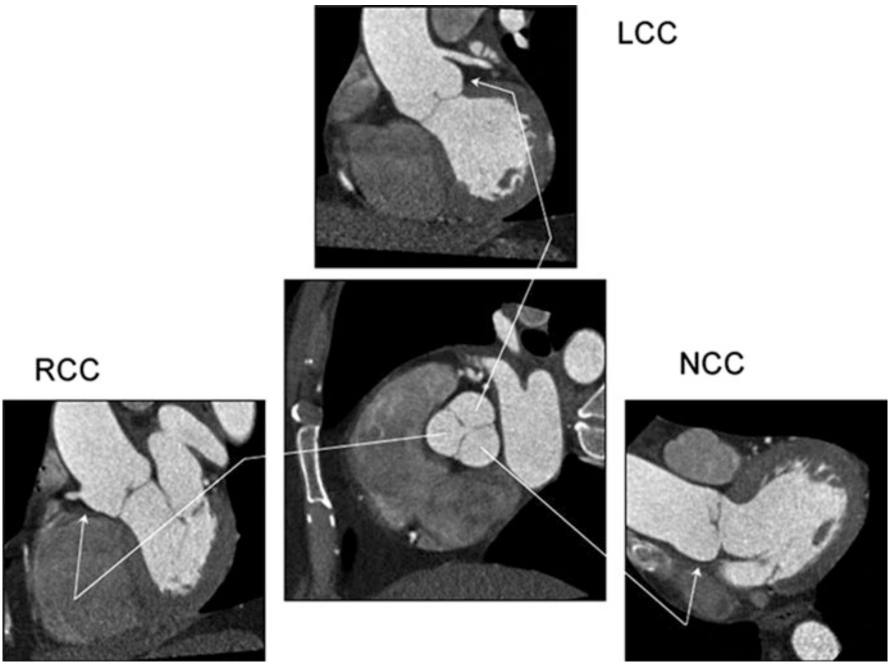

Fig. 8.3 Relationship between aortic valve cusps and coronary ostia. The central panels show a cross section through the aortic root with the three aortic valve cusps. The three surrounding panels show oblique sagittal images of each cusp. *LCC,* left coronary cusp; *RCC,* right coronary cusp; *NCC,* non-coronary cusp

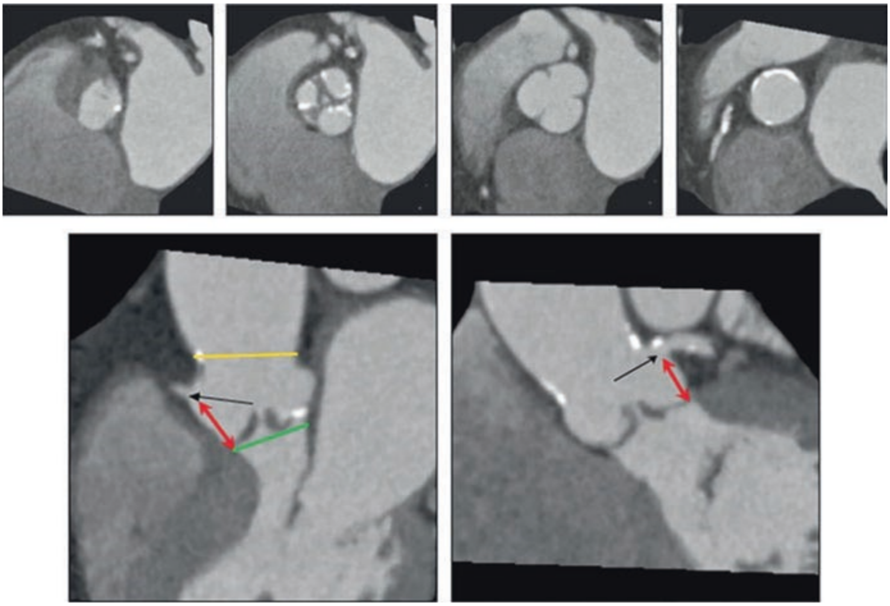

Fig. 8.4 Aortic root, aortic valve, and coronary ostia. The upper panels show (*left* to *right*) cross sections at the "aortic annulus," aortic valve, sinuses of Valsalva, and sinotubular junction. There is moderate thickening and calcification of the aortic valve leaflets

8.2.1.2 Imaging

The position of the aortic root relative to the body axis and corresponding alignment of the X-ray plane are critically important for precise placement of the valve. With angiography, overlap-free visualization of the three coronary cusps, which are oriented along the aortic valve plane, typically requires caudal angulation in the RAO projection and cranial angulation in the LAO projection. The current standard approach is based on the identification of X-ray root angiograms (using a pigtail catheter in either the non-coronary cusp or right coronary cusp depending on the type of valve being used) in one or preferably two orthogonal planes prior to the procedure after repeated root injections. Pre-procedural multi-detector CT data of the aortic root allow prediction of the optimal angulation of the root angiogram, which facilitates the angiographic procedure and reduces the number of root injections (Fig. 8.5) [84, 85]. In cases of TAVI within a prior surgical or transcatheter bioprosthetic aortic valve (i.e., "valve-in-valve"), X-ray fluoroscopy alone can be used to identify the bottom aortic annulus (coplanar view), obviating the need for aortic root angiograms during positioning and deployment of the transcatheter heart valve [86].

As described above, using imaging modalities, the annulus plane is defined as the plane created by the lowest hinge point of the three leaflets of the aortic valve ("inferior virtual basal ring") (Figs. 8.2 and 8.4). Detailed 3D analysis demonstrates

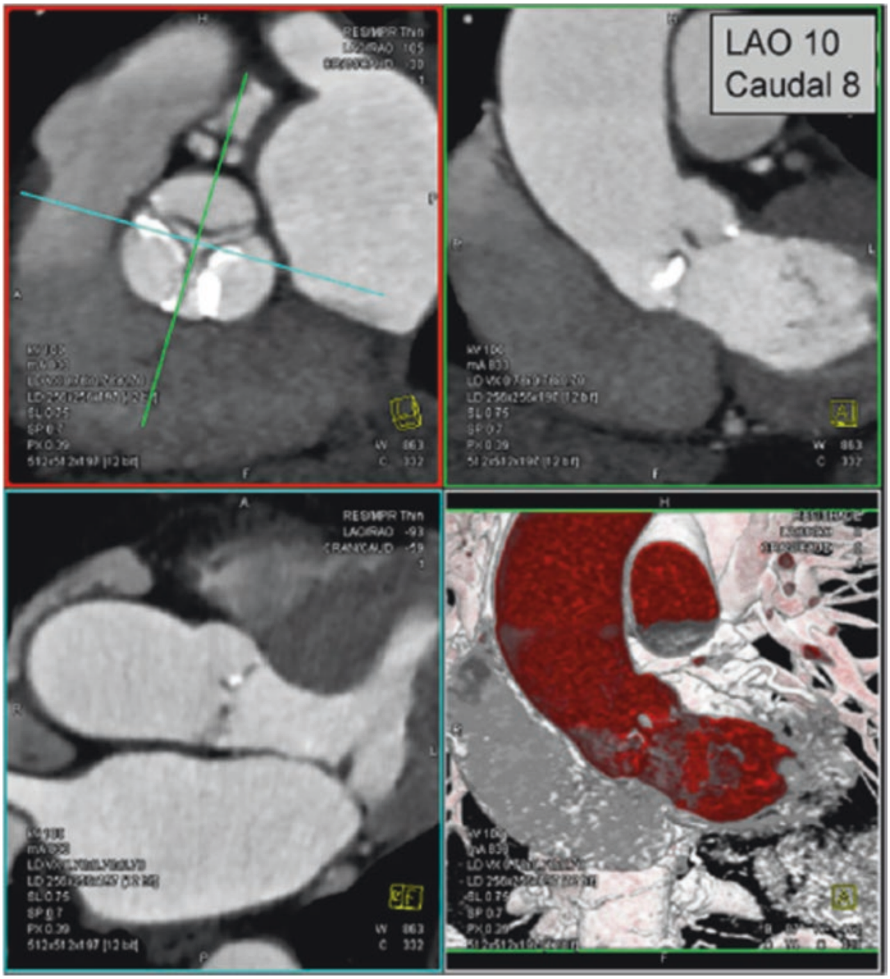

Fig. 8.5 Prediction of angiographic planes for transcatheter aortic valve implantation. In a double-oblique reconstructed image, the crosshair of the cut planes is centered on the aortic valve (*left upper panel*) and rotated to obtain images of the aortic root, described in angiographic coordinates/planes (*right upper panel*)

that this clinically defined annulus is typically elliptical [87–97], and therefore, maximal and minimal annular diameters are reported with CT. Mean annular diameter by CT correlates best but is typically slightly larger than that obtained with TEE. Despite this, CT is now the most commonly used method for valve sizing/selection (based on the aortic annulus area or perimeter) given its superiority in clinical outcomes compared to echocardiography [98]. Measurement of the distance between the coronary arteries, artery ostia, and distal tip of the aortic valve leaflets is important and can be derived from angiography, CT, and TEE (Fig. 8.4). In the case of a low ostium or a long leaflet, there is increased risk of coronary (particular left main) occlusion [87, 89, 90, 94]. This information is vital intra-procedurally such that operators can prepare for coronary protection in advanced. Coronary re-access can be challenging due to a multitude of reasons, including native leaflet obstruction, stent frame position, and mal-aligned commissures [99]. Studies have shown this to be particularly more challenging in self-expanding valves compared to balloon-expandable valves [100]. Due to this, special device advancement techniques have been utilized and validated to significantly reduce the occurrence of commissural overlap with the coronary ostium and thereby theoretically increase success of coronary re-access if needed [101]. A special leaflet laceration technique called BASILICA (Bioprosthetic or native Aortic Scallop Intentional Laceration to prevent Iatrogenic Coronary Artery obstruction during TAVR) has been shown to be feasible and safe to prevent coronary artery obstruction from TAVR in high-risk patient subsets [102].

Imaging allows detailed description of the presence and distribution of valve and root calcification (Fig. 8.6) [103–109]. For example, calcification frequently extends from the aortic valve commissures to the base of the anterior mitral leaflets and sinotubular junction. The amount and distribution of calcification in the proximal device landing zone at the annulus can affect sealing of the prosthesis, leading to paravalvular regurgitation post-valve deployment. Aortic calcification of the sinotubular junction can influence precise placement of the valve during TAVI by restricting balloon expansion and potentially leading to the ventricular displacement of

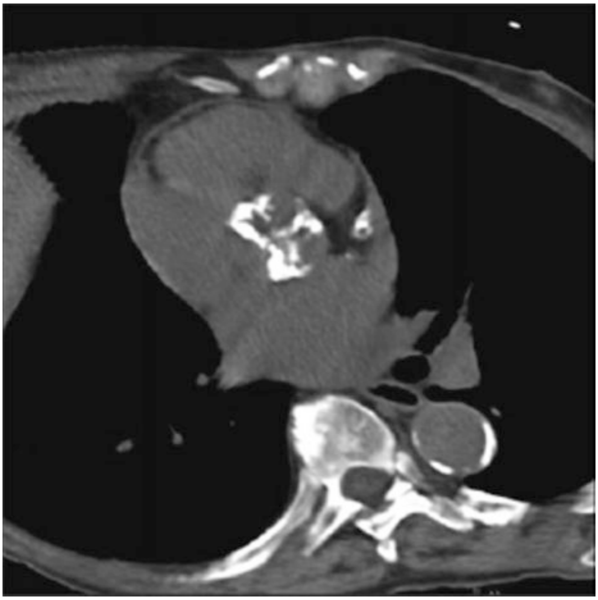

Fig. 8.6 Dense calcification of aortic valve. In this image of a non-contrast-enhanced scan, dense calcification is seen along all three aortic valve cusps. This pattern suggests a tricuspid valve. Using calcium scoring software, the extent of calcification can be quantified

device at the time of deployment. Presence of eccentric or calcified nodules can also increase the risk of rare, but catastrophic peri-procedural complications such as aortic annular rupture or ventricular septal defects. Lastly, the extent and quantification of aortic calcification using calcium scoring software (and using sex-specific thresholds of the Agatston score) can assist clinically with the diagnosis of severe aortic stenosis in difficult or ambiguous cases.

Direct observation of the aortic valve opening area allows for correlation of the pattern of valve opening with leaflet anatomy and leaflet calcification. Direct planimetry of the aortic valve opening area with CT has been shown to provide reproducible results in comparison with TEE and MRI (Fig. 8.7) [110–117].

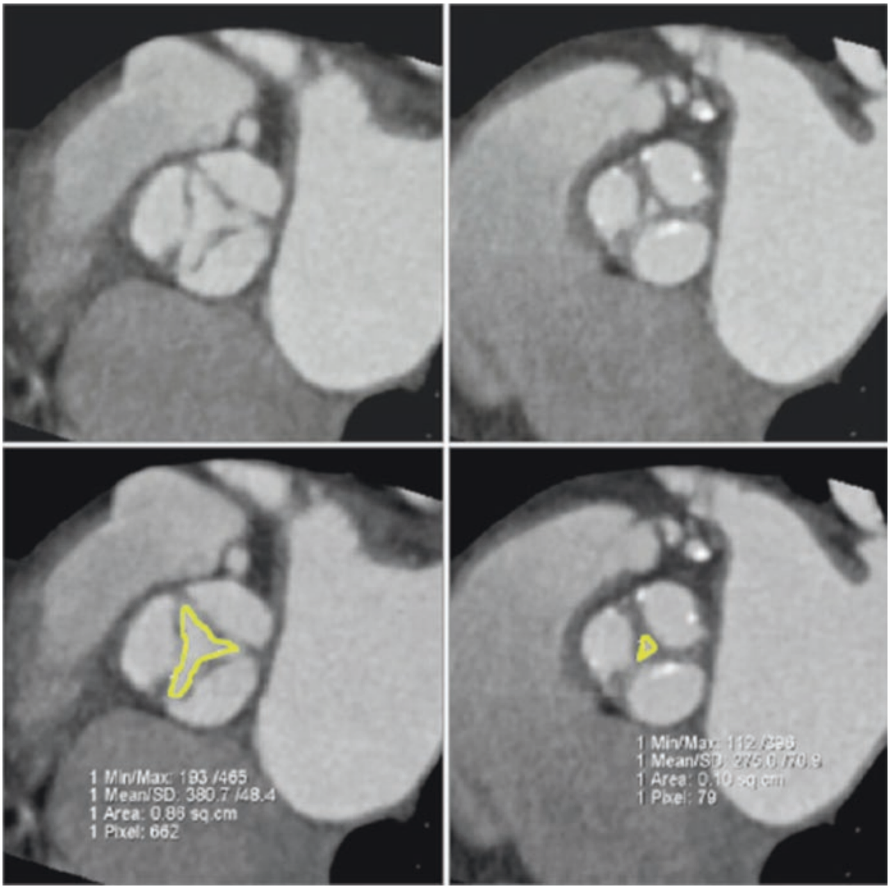

Fig. 8.7 Image reconstruction in systolic and diastolic phase of the cardiac cycle. Image reconstruction in systolic (*left*) and diastolic (*right*) phase of the cardiac cycle demonstrates restricted systolic opening and incomplete diastolic coaptation, consistent with moderate aortic stenosis and mild insufficiency, respectively

During periprocedural 3D TEE, the biplane imaging mode is valuable in simultaneously imaging the aortic valve in both the short- and long-axis views, both in 2D and in color Doppler (Fig. 8.8). This allows the accurate positioning of the prosthetic device in the center of the stenotic valve in both orientations, as well as rapidly localizing post-implantation paravalvular regurgitation. However, the trend has been moving away from general anesthesia, and more toward conscious sedation, hence decreasing the usage of intra-procedural TEE. Transthoracic echocardiogram, aortic root angiography, and/or hemodynamics are now the most commonly used assessments for post-implantation paravalvular regurgitation.

8.2.2 Transcatheter Mitral Valve Procedures

8.2.2.1 Anatomy

The annulus of the mitral valve is an oval, saddle-shaped structure which is formed by continuity of the left atrial tissue with the left ventricular tissue, as well as the base of the mitral valve leaflets (Figs. 8.9 and 8.10) [118, 119]. The mitral valve apparatus consists of the annulus, leaflet, chordae, and the papillary muscles (the anteromedial and posterolateral papillary muscles). The annulus is divided into anterior and posterior parts by the commissures.

The anterior leaflet is larger in length but covers only about one-third of the circumference of the annulus. The posterior leaflet is shorter in length but covers approximately two-third of the annulus. The chordae arise from the papillary muscle tips and then span to the leaflets in a fan-shaped manner (Fig. 8.11). There are two main chordae arising from each head of the papillary muscle, reaching each of the leaflets. However, there is a considerable variation in the origin and distribution of the chordae.

The coronary sinus (CS) extends along the left atrioventricular groove close to the mitral annulus and drains into the right atrium. In the context of sinus annuloplasty procedures, a major concern is the close proximity of the CS to the left circumflex artery (LCX) and the potential risk of CS-based devices potentially impinging on the LCX [120]. See Chap. 1 for more information on the anatomy of the atrioventricular valves.

8.2.2.2 Imaging

Three-dimensional imaging allows a detailed understanding of the mitral valve apparatus including the mitral annulus and leaflets and has been extensively described with echocardiography [121–126]. Description of mitral valvular anatomy is critical for procedures involving the mitral leaflets, including mitral valve repair/replacement procedures and percutaneous closure of paravalvular regurgitation. Real-time 3D and full-volume acquisition with TEE allows imaging of the

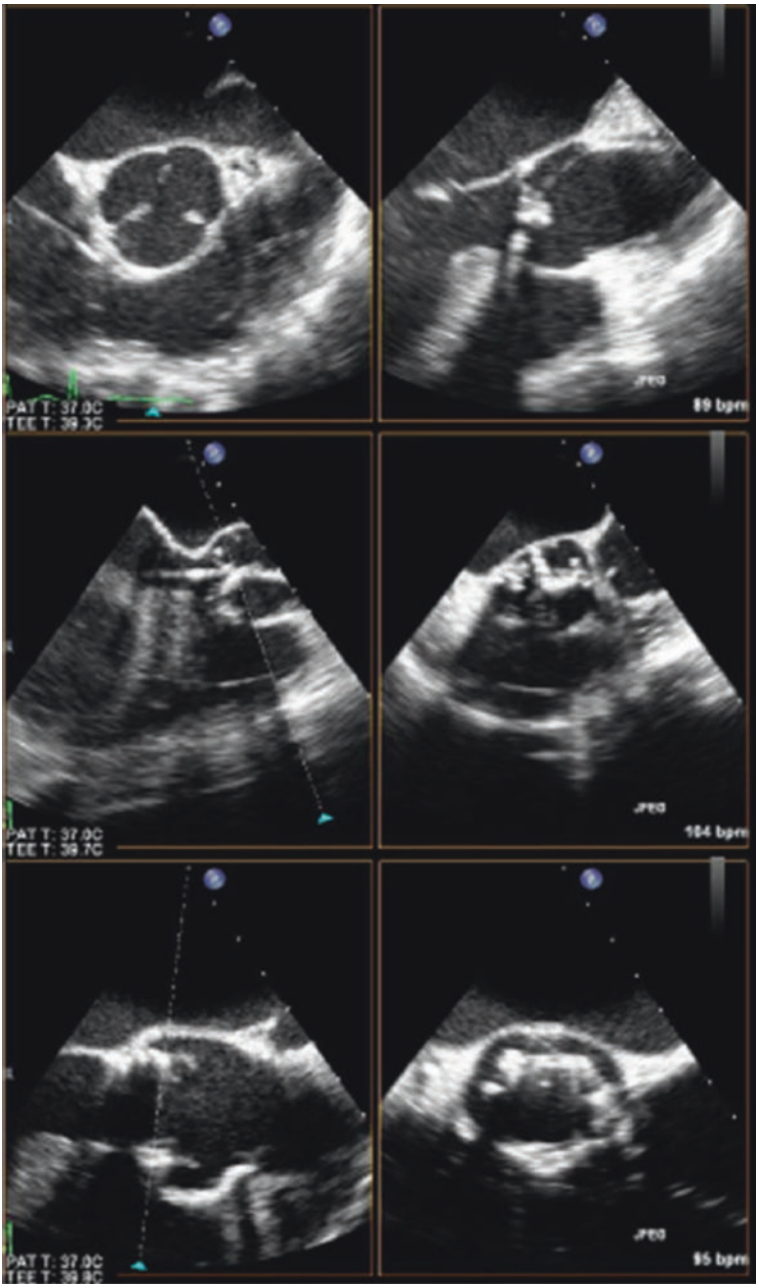

Fig. 8.8 Biplane real-time three-dimensional (3D) echocardiography. Biplane real-time imaging of a patient with severe aortic stenosis undergoing transcatheter aortic valve implantation (TAVI), in both short and long axis, before (*top panel*), during (*middle panel*), and after (*bottom panel*) device deployment. Simultaneous imaging of the aortic valve in two planes in high spatial and temporal resolution is crucial for the precise positioning of the prosthetic device in TAVI

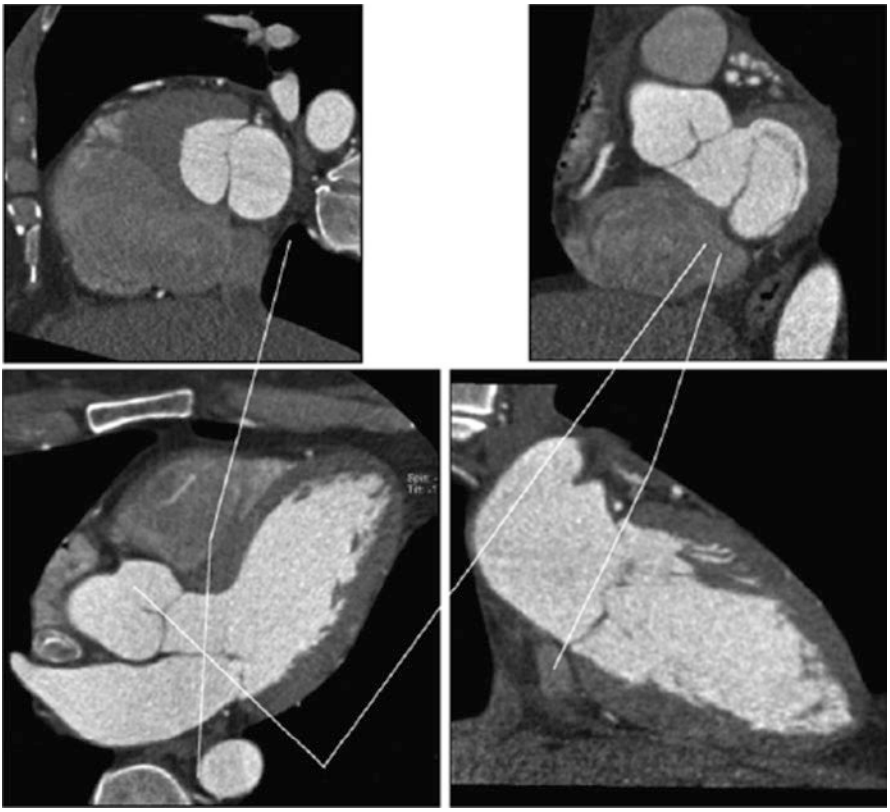

Fig. 8.9 Relationship between LVOT, anterior mitral leaflet, and mitral annulus. The upper panels show (*left* to *right*) cross sections of the LVOT/anterior mitral leaflet and mitral annulus. The close relationship of the structures is demonstrated

entire mitral valve and annulus over full cardiac cycles [47, 127–130]. Therefore, 3D echocardiography is a critical part of the pre-procedural assessment of patients with mitral regurgitation and allows clarification of etiology (i.e., degenerative versus functional mitral regurgitation), determination of severity, and assessment of amenability of the mitral valve to percutaneous procedures and pre-procedural planning (Fig. 8.12). For periprocedural guidance, full-volume 3D echocardiography data acquisition is less useful because of the need for offline analysis. However, real-time 3D echocardiography with its enface mitral valve view from the left atrium similar to the surgeon's view, as well as simultaneous biplane imaging with its high temporal and spatial resolutions both in 2D and in color Doppler modes, is invaluable for procedures such as mitral valve clip (Fig. 8.13) and percutaneous closure of paravalvular regurgitation (Fig. 8.14). Specifically, the 3D enface mitral valve view is particularly useful for orientation of the mitral valve clip device. Biplane imaging in the 2D echocardiography mode is particularly useful for medial/lateral and anterior/posterior orientation and is the key view for leaflet grasping. In addition, 2D

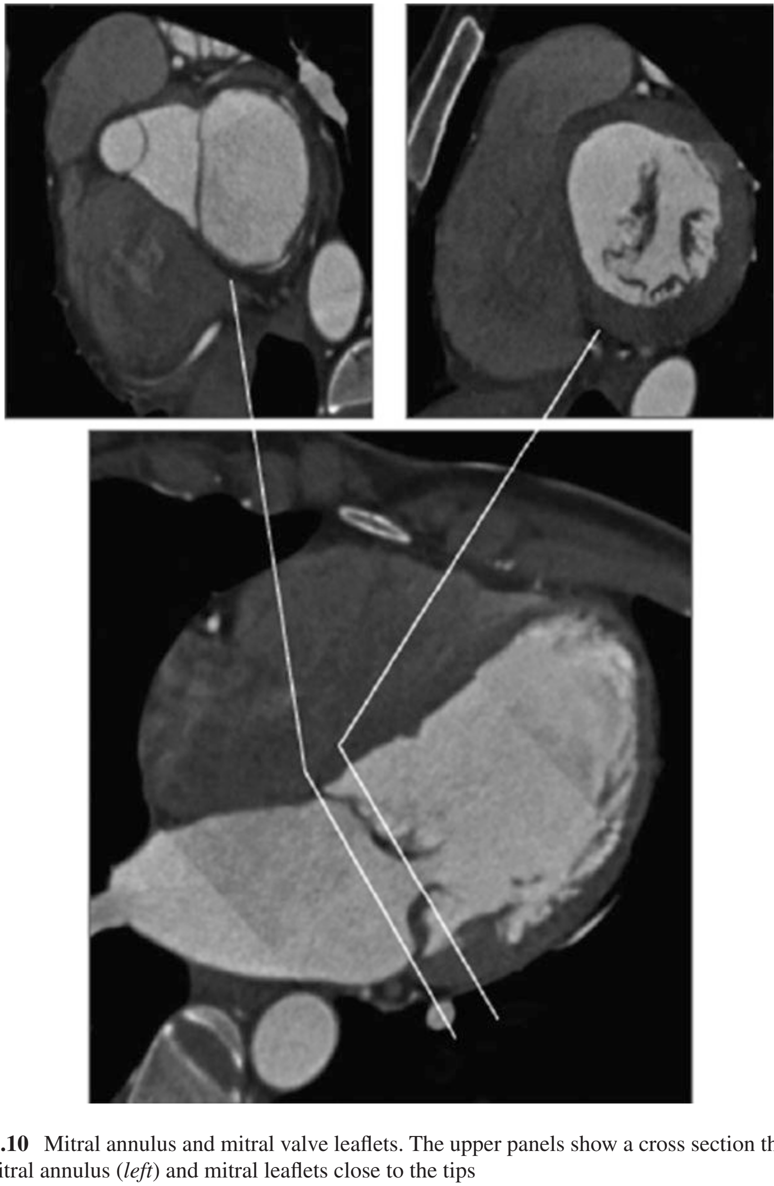

Fig. 8.10 Mitral annulus and mitral valve leaflets. The upper panels show a cross section through the mitral annulus (*left*) and mitral leaflets close to the tips

biplane imaging is crucial for the trans-septal puncture (crossing from the right atrium into the left atrium), which is a crucial procedural step to the mitral valve clip device and other transcatheter mitral valve replacement (TMVR) procedures.

Similar to TAVI, CT is essential for annular sizing in TMVR. The typical measurements obtained from CT include the annular: projected area, perimeter, intercommissural, septal-lateral, and trigone-trigone distances [131]. Depending on the

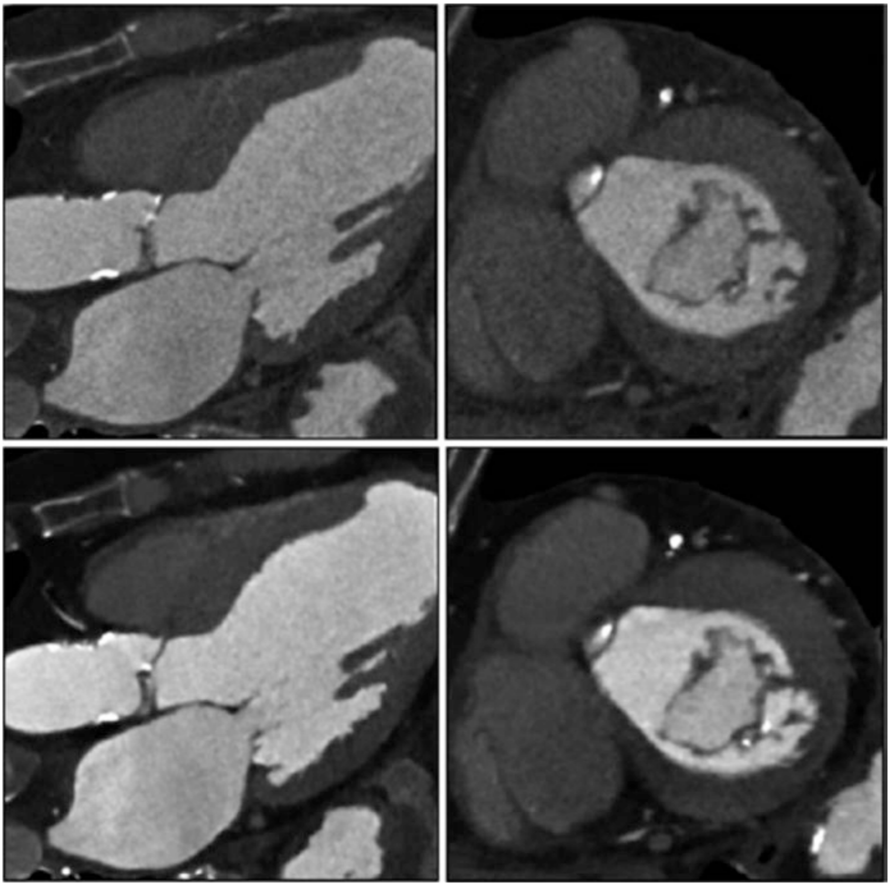

Fig. 8.11 Mitral leaflets, mild mitral annular calcification, and papillary muscles. In this image, mild mitral annular calcification is seen in the infero-lateral aspect of the annulus. The images also show the posterior papillary muscles and chordae tendineae. The images are reconstructed with standard “filtered back projection” (*upper panels*) and “iterative reconstruction” (*lower panels*). Iterative reconstruction is associated with significantly decreased image noise

device selected for use, different variables/parameters are used for sizing. Three-dimensional TEE sizing of the mitral annulus can also be used as well, with the added benefit of the high temporal resolution providing information on the dynamics and function of the mitral annulus. CT and echocardiography are also helpful in evaluating the transapical access point, ideal intercostal access site, annular landing zone, presence of calcification (i.e., mitral annular calcification), fluoroscopic coplanar angles, and prediction of left ventricular outflow tract (LVOT) obstruction post-procedure [132]. This is helpful in cases of transcatheter valve-in-valve, valve-in-ring, valve-in-mitral annular calcification, or TMVR. For any type of implantation in the mitral position, post-procedural LVOT obstruction is a concern and CT simulations (along with aortomitral angulation, left ventricular cavity size,

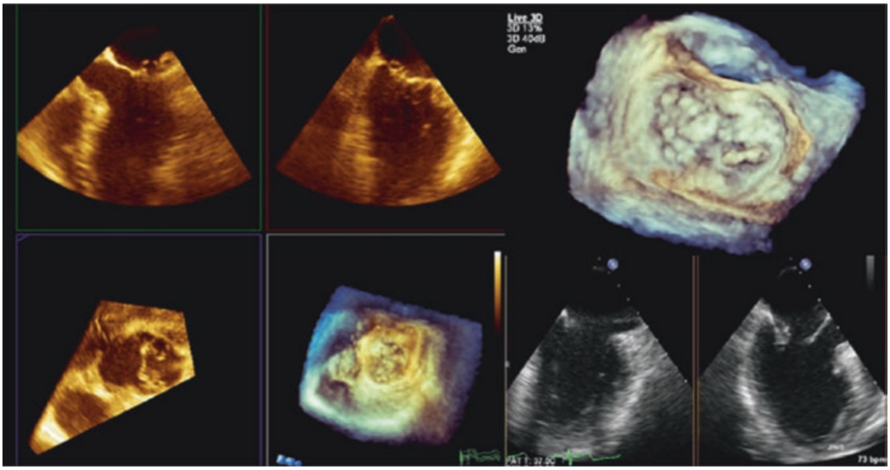

Fig. 8.12 Three-dimensional echocardiography assessment of a patient with severe mitral regurgitation. With the full-volume 3D acquisition, offline analysis of the data set accurately identifies the posterior mitral leaflet medial flail segment (*left panel*). Real-time 3D acquisitions also visualize the posterior medial flail segment with an enface view of the mitral valve from the left atrium, similar to the surgeon's view of the mitral valve (*top right panel*). Simultaneous biplane imaging of the mitral valve allows the assessment of the flail segment in high temporal and spatial resolution, both in two-dimensional (2D) and in color Doppler modes (*bottom right panel*). The medial location of the flail segment near the commissure makes it challenging for percutaneous treatment

interventricular septal size) can be used to predict the risk in patients being evaluated for TMVR. A technique similar to BASILICA for prevention of coronary obstruction in TAVR has been developed for TMVR called LAMPOON (Laceration of the Anterior Mitral leaflet to Prevent Outflow Obstruction) technique and has been shown to be effective in preventing and treating LVOT obstruction [133]. Two-dimensional and three-dimensional echocardiography are vital intra-procedurally to assist with trans-septal puncture, trans-apical cannulation, guidewire and device positioning/functioning, assessment of paravalvular leak, device seating and stability, and LVOT obstruction [132]. Figure 8.15 depicts fluoroscopic images of mitral valve-in-valve, valve-in-ring- and valve-in-mitral annular calcification, respectively.

For CS-related procedures, fluoroscopy, CT, and TEE are helpful for proper positioning of the device and evaluating the effectiveness of the intervention. Several studies have used angiography and CT to describe the in vivo anatomical relationships between mitral annulus and CS as well as CS and LCX [134–137]. These studies observed significant variance of CS to mitral annulus separation. The LCX crossed between the CS and mitral annulus in 74–97% of patients at a variable distance from the ostium of CS, depending on coronary dominance. In addition, obtuse marginal branches and posterolateral branches were also in a position to potentially be compressed by a device placed within the CS. Therefore, evaluation of the relationship between the CS/great cardiac vein and the LCX is an important factor in determining the safety of CS-based devices.

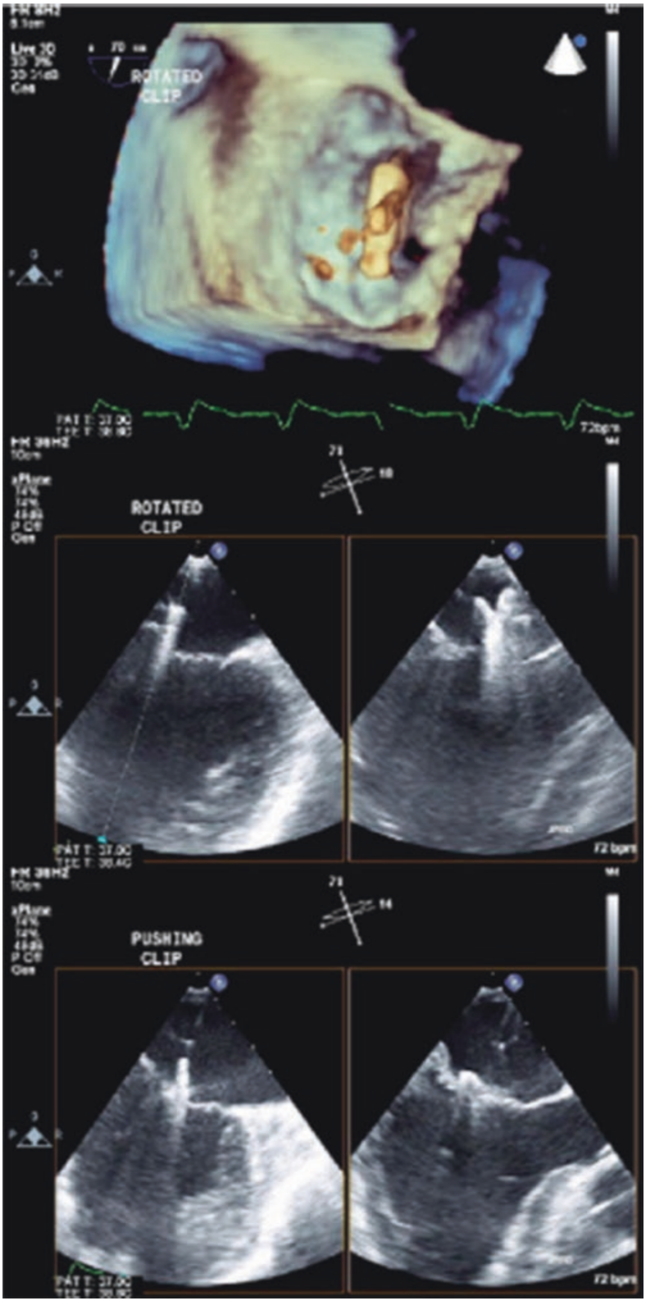

Fig. 8.13 Three-dimensional echocardiography and mitral valve clip. In the mitral valve clip procedure, real-time 3D echocardiography identifies the position of the clip with respective to the mitral valve, in the enface perspective (*top panel*). The accurate positioning of the mitral clip often relies on simultaneous biplane imaging that more precisely defines the relationship between the arms of the clip with the valve leaflets (*bottom panel*)

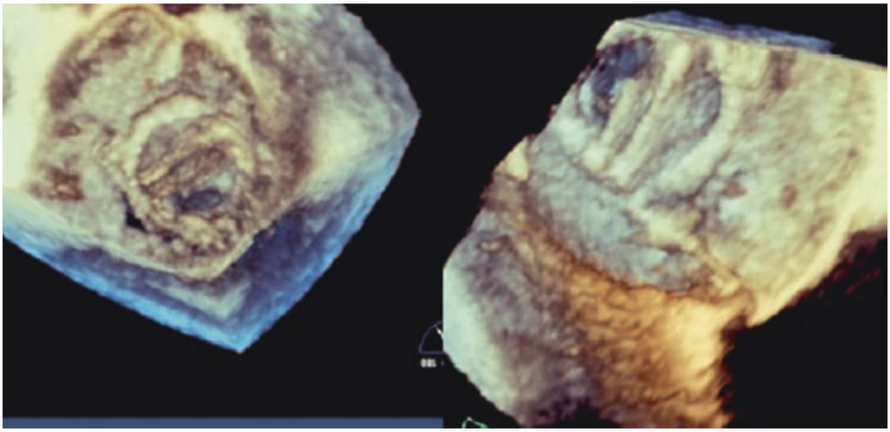

Fig. 8.14 Three-dimensional echocardiography and percutaneous closure of paravalvular leaks. The enface view of the mitral valve obtained by real-time 3D echocardiography is especially important in the percutaneous closure of prosthetic paravalvular mitral regurgitation, as it provides the interventionist an anatomical orientation of the paravalvular regurgitation and the valve leaflets and surrounding structure. In this example, the defect is identified in the posterior aspect of the mitral prosthesis (*left panel*). In combination with other 2D and color Doppler views, a guidewire is successfully passed through the defect with subsequent successful deployment of the closure device (*right panel*)

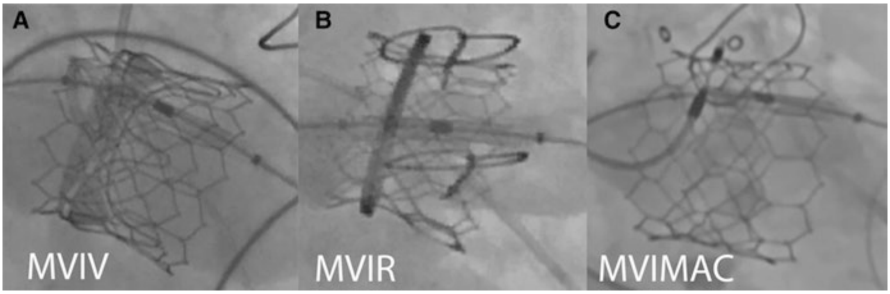

Fig. 8.15 Fluoroscopic Images of mitral: (**a**) valve-in-valve, (**b**) valve-in-ring, and (**c**) valve-in-mitral annular calcification

For all transcatheter valvular procedures, assessment of vascular access is important and relies on different imaging modality (Fig. 8.16). Absolute size, amount, and extent of calcification, as well as tortuosity of iliac and femoral artery determine suitability for the procedure [138, 139]. Vascular complications are the major cause of morbidity and mortality in patients undergoing TAVI, and this should therefore be considered as transcatheter valve procedures increase in number with an expansion toward lower-risk, younger patients.

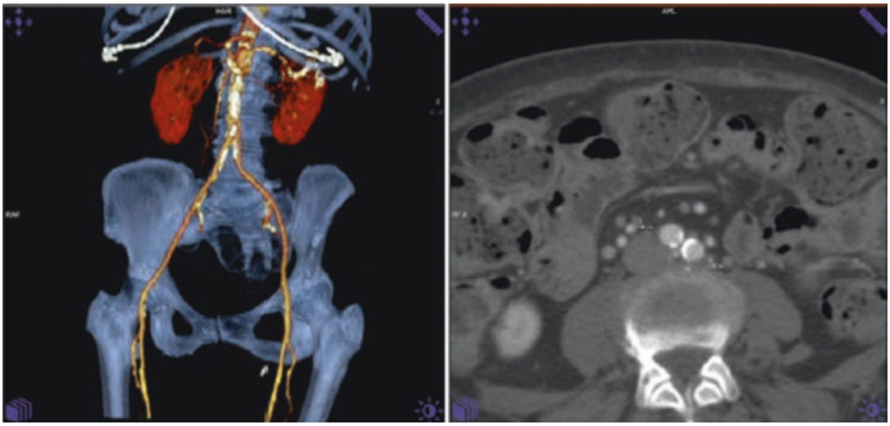

Fig. 8.16 Assessment of vascular access. Computed tomography allows assessment of the iliac anatomy including vessel diameter, calcification, and tortuosity

8.2.3 Transcatheter Tricuspid Valve Procedures

8.2.3.1 Anatomy

The tricuspid valve (TV) is the most anterior and apical of the four cardiac valves, and its apparatus is composed of leaflets, chordae and papillary muscles, annulus, and surrounding structures [140–142]. The valve leaflet orifice area is typically large at 7–9 cm^2 and with a low diastolic pressure gradient across the valve between the right atrium (RA) and right ventricle (RV) (mean gradient < 2 mmHg). The number of tricuspid leaflets is variable, but most commonly consists of an anterior, posterior, and septal leaflet; usually of unequal size, with anatomical variations of > 3 leaflets being present not being uncommon. The anterior leaflet is usually the largest, longest, and the most mobile of the three leaflets while the septal leaflet is the shortest in the radial direction and the least mobile. The posterior leaflet may have multiple scallops depending on anatomic variations. Overall, the leaflets are very thin and translucent which may be less ideal for anchoring interventional devices.

There are typically two papillary muscles with an occasional variant third. The anterior papillary muscle is the largest, located along the anterolateral RV wall, and provides chordae support to the anterior and posterior leaflets. The posterior papillary muscle provides chordae to the posterior and septal leaflets. The third variable septal papillary muscle may be present, absent, or even multiple. Chordae may even arise directly from the interventricular septum attaching to the anterior and septal leaflets, as well as other locations such as the RV free wall or moderator band.

The tricuspid annulus lacks a robust fibrous structure, is D-shaped (flat along the septum), and nonplanar. Due to this, annular dilation typically occurs laterally and posteriorly where there is lack of fibrous tissue. Coaptation of the TV leaflets occurs at the level or just below the annulus. The tricuspid annulus is dynamic, with significant changes in area size depending on phase in the cardiac cycle and volume loading conditions.

Surrounding structures to the TV include the non-coronary sinus of Valsalva near the anteroseptal commissure, atrioventricular (AV) node and Bundle of His near the septal leaflet attachment, right coronary artery (RCA) which courses in the AV groove, and the superior vena cava (SVC) and inferior vena cava (IVC) which are potential therapeutic targets. Awareness of these structures is important as they can be inadvertently damaged during transcatheter tricuspid valve interventions leading to significant complications, morbidity, and mortality.

8.2.3.2 Imaging

Pre-procedural and intra-procedural imaging are vital to transcatheter TV interventions. Two-dimensional and three-dimensional imaging is useful in pre-procedural planning using various modalities (i.e., echocardiography, computed tomography, and cardiac magnetic resonance imaging) [143]. Imaging is imperative to evaluate severity of pathology, tricuspid annulus size, leaflet coaptation/tethering, and etiology. Pre-procedural echocardiography is essential to assess amenability and feasibility. Sometimes the tricuspid valve may be difficult to image from an echocardiographic standpoint due to the anterior location of the valve; hence, feasibility is partially based on image quality suitable for intra-procedural guidance. Important measurements include RA & RV dimensions/areas and function, tricuspid annulus dimensions (i.e., antero-posterior/septal-lateral diameter, perimeter, area, RV apex-annulus distance), calcification, relationship and distance of the RCA to the tricuspid annulus, leaflet tethering height, coaptation gap, distance, tenting area and volume, subvalvular apparatus, and IVC/SVC dimensions [144, 145]. Similar to TAVI and TMVR, pre-procedural CT is essential in obtaining measurements to choose the optimal tricuspid intervention device.

TV edge-to-edge repair is currently the most commonly used and shown to be an effective method for transcatheter-based treatment of severe tricuspid regurgitation [140, 146, 147]. TV edge-to-edge repair cannot be possible without TEE guidance intra-procedurally. Both 2D (with biplane imaging) and 3D echocardiography are essential intra-procedurally to guide the clip device to the TV (making sure to avoid puncture of the inter-atrial septum), clip positioning and grasping of leaflets, evaluate for device stability and efficacy after clip deployment, and assess for any adverse complications during and post-procedure (i.e., pericardial effusion). Specifically, 3D TEE enface view in the deep transgastric position is used for clip orientation, and 2D TEE biplane imaging in the mid or deep esophageal position is often used for leaflet grasping. Other views are used to verify or confirm adequate tissue grasp before full deployment of the clips. Typically, approximation of the edges of the anterior and septal leaflets together has been associated with the best outcomes; however, each case is tailored based on the etiology of pathology.

There are several other transcatheter tricuspid interventional devices (annular reduction devices, heterotopic caval valve implantation, valve-in-valve transcatheter valve replacement, and total tricuspid valve replacement) that are still under clinical investigation. Similar to the edge-to-edge repair device, intra-procedural 2D & 3D TEE guidance is imperative to device implantation and success. Given the rapid advancement of these technologies and current clinical investigation, the optimal techniques and intra-procedural imaging protocols are yet to be determined.

8.3 From Bench to Bedside: Imaging and Device Design/Development

Beyond its value for clinical decision-making in the individual patient, 3D data are increasingly used for device design [148, 149]. Advances in medical imaging and computational modeling allow simulation of physiological conditions in patient-specific 3D vascular models. Such models can account for the unique features of the human circulation with appropriate 3D anatomical and physiological input data. This approach will allow prospective design of devices. Computed tomography is particularly attractive, because it acquires high-resolution volumetric data sets with sufficient temporal resolution for multiphasic analysis [150]. Along with high spatial resolution, newer state-of-the-art multi-detector CT systems have improved temporal resolutions and allow for quantification of the anatomy at multiple points in the cardiac cycle and subsequent mathematical modeling [151].

Finite element analysis is widely used in clinical research and device development. Finite element models quantitate the effects of changes in one or more of the parameters characterizing the system, including geometrical dimensions, mechanical properties, and fluid dynamics. The reliability of the results obtained through finite element modeling depends on the degree of realism achieved in modeling the physical characteristics that affect valvular biomechanics, including geometry, tissue mechanical properties, and boundary conditions due to the interaction with the surrounding tissues.

Models derived from in vivo 3D imaging provide realistic data. For example, finite element analysis using real-time 3D echocardiography examined regional mitral annular geometry and demonstrated that the nonplanar shape of the mitral annulus diminishes mitral leaflet stress [152]. Three-dimensional finite element models were also developed based on MRI of normal human aortic valve and root [153].

Computational methodology simulating valve systems is an integral part of valve design. The Food and Drug Administration in the United States and similar regulatory bodies in the European Community have established detailed guidelines for in vitro and in vivo preclinical testing of heart valve prostheses, with standardized methods and equipment in assessing fatigue, flow dynamics, and hydrodynamics of valve implants [154–156].

Direct clinical application has been described in the context of implantation of a new percutaneous pulmonary valve into a dilated pulmonary trunk, using patient-specific data to influence the design of the device and ensure patient safety [157–160].

8.4 Conclusion

Transcatheter procedures for valvular and structural heart disease require multimodality imaging both for preoperative planning and direct guidance. Imaging modalities include 2D modalities, such as fluoroscopy and 2D echocardiography, as well as 3D imaging modalities, including CT, MRI, C-arm CT, and 3D echocardiography, which acquire volumetric data sets and allow subsequent 3D display and visualization in unlimited planes. The data described above suggest an emerging role of 3D imaging for novel surgical and transcatheter approaches including device design.

References

1. Iung B, Baron G, Butchart EG et al (2003) A prospective survey of patients with valvular heart disease in Europe: the Euro heart survey on valvular heart disease. Eur Heart J 24:1231–1243
2. Mihaljevic T, Nowicki ER, Rajeswaran J et al (2008) Survival after valve replacement for aortic stenosis: implications for decision making. J Thorac Cardiovasc Surg 135:1270–1278
3. Varadarajan P, Kapoor N, Bansal RC et al (2006) Clinical profile and natural history of 453 nonsurgically managed patients with severe aortic stenosis. Ann Thorac Surg 82:2111–2115
4. Pai RG, Kapoor N, Bansal RC et al (2006) Malignant natural history of asymptomatic severe aortic stenosis: benefit of aortic valve replacement. Ann Thorac Surg 82:2116–2122
5. Kapadia SR, Goel SS, Svensson L et al (2009) Characterization and outcome of patients with severe symptomatic aortic stenosis referred for percutaneous aortic valve replacement. J Thorac Cardiovasc Surg 137:1430–1435
6. Cribier A, Eltchaninoff H, Tron C et al (2004) Early experience with percutaneous transcatheter implantation of heart valve prosthesis for the treatment of end-stage inoperable patients with calcific aortic stenosis. J Am Coll Cardiol 43:698–703
7. Grube E, Schuler G, Buellesfeld L et al (2007) Percutaneous aortic valve replacement for severe aortic stenosis in high-risk patients using the second and current third-generation self-expanding CoreValve prosthesis: device success and 30-day clinical outcome. J Am Coll Cardiol 50:69–76
8. Lichtenstein SV, Cheung A, Ye J et al (2006) Transapical transcatheter aortic valve implantation in humans: initial clinical experience. Circulation 114:591–596
9. Webb JG, Pasupati S, Humphries K et al (2007) Percutaneous transarterial aortic valve replacement in selected high-risk patients with aortic stenosis. Circulation 116:755–763
10. Petronio AS, De Carlo M, Bedogni F et al (2010) Safety and efficacy of the subclavian approach for transcatheter aortic valve implantation with the CoreValve revalving system. Circ Cardiovasc Interv 3:359–366
11. Krishnaswamy A, Tuzcu EM, Kapadia SR (2010) Update on transcatheter aortic valve implantation. Curr Cardiol Rep 12:393–403

12. Gurvitch R, Wood DA, Tay EL et al (2010) Transcatheter aortic valve implantation: durability of clinical and hemodynamic outcomes beyond 3 years in a large patient cohort. Circulation 122:1319–1327
13. Eltchaninoff H, Prat A, Gilard M et al (2010) Transcatheter aortic valve implantation: early results of the FRANCE (FRench Aortic National CoreValve and Edwards) registry. Eur Heart J 32:191–197
14. Leon MB, Smith CR, Mack M et al (2010) Transcatheter aortic-valve implantation for aortic stenosis in patients who cannot undergo surgery. N Engl J Med 363:1012–1015
15. Alfieri O, Maisano F, De Bonis M et al (2001) The double-orifice technique in mitral valve repair: a simple solution for complex problems. J Thorac Cardiovasc Surg 122:674–681
16. Maisano F, Torracca L, Oppizzi M et al (1998) The edge-to-edge technique: a simplified method to correct mitral insufficiency. Eur J Cardiothorac Surg 13:240–245
17. St Goar FG, Fann JI, Komtebedde J et al (2003) Endovascular edge-to-edge mitral valve repair: short-term results in a porcine model. Circulation 108:1990–1993
18. Silvestry FE, Rodriguez LL, Herrmann HC et al (2007) Echocardiographic guidance and assessment of percutaneous repair for mitral regurgitation with the Evalve MitraClip: lessons learned from EVEREST I. J Am Soc Echocardiogr 20:1131–1140
19. Feldman T, Wasserman HS, Herrmann HC et al (2005) Percutaneous mitral valve repair using the edge-to-edge technique: six-month results of the EVEREST phase I clinical trial. J Am Coll Cardiol 46:2134–2140
20. Feldman T, Kar S, Rinaldi M et al (2009) Percutaneous mitral repair with the MitraClip system: safety and midterm durability in the initial EVEREST (Endovascular Valve Edge-to-Edge REpair Study) cohort. J Am Coll Cardiol 54:686–694
21. Webb JG, Harnek J, Munt BI et al (2006) Percutaneous transvenous mitral annuloplasty: initial human experience with device implantation in the coronary sinus. Circulation 113:851–855
22. Maniu CV, Patel JB, Reuter DG (2004) Acute and chronic reduction of functional mitral regurgitation in experimental heart failure by percutaneous mitral annuloplasty. J Am Coll Cardiol 44:1652–1661
23. Kaye DM, Byrne M, Alferness C et al (2003) Feasibility and short-term efficacy of percutaneous mitral annular reduction for the therapy of heart failure-induced mitral regurgitation. Circulation 108:1795–1797
24. Schofer J, Siminiak T, Haude M et al (2009) Percutaneous mitral annuloplasty for functional mitral regurgitation: results of the CARILLON Mitral Annuloplasty Device European Union Study. Circulation 120:326–333
25. Eicken A, Ewert P, Hager A et al (2011) Percutaneous pulmonary valve implantation: two centre experience with more than 100 patients. Eur Heart J 32:1260–1265
26. Zahn EM, Hellenbrand WE, Lock JE et al (2009) Implantation of the melody transcatheter pulmonary valve in patients with a dysfunctional right ventricular outflow tract conduit early results from the US Clinical trial. J Am Coll Cardiol 54:1722–1729
27. Lauten A, Ferrari M, Hekmat K et al (2011) Heterotopic transcatheter tricuspid valve implantation: first-in-man application of a novel approach to tricuspid regurgitation. Eur Heart J 32:1207–1213
28. Webb JG, Wood DA, Ye J et al (2010) Transcatheter valve-in-valve implantation for failed bioprosthetic heart valves. Circulation 121:1634–1636
29. Nunez-Gil IJ, Goncalves A, Rodriguez E et al (2011) Transapical mitral valve-in-valve implantation: a novel approach guided by three-dimensional transesophageal echocardiography. Eur J Echocardiogr 12:335–337
30. Vahanian A, Alfieri O, Al-Attar N et al (2008) Transcatheter valve implantation for patients with aortic stenosis: a position statement from the European Association of Cardio-Thoracic Surgery (EACTS) and the European Society of Cardiology (ESC), in collaboration with the European Association of Percutaneous Cardiovascular Interventions (EAPCI). Eur Heart J 29:1463–1470

31. Kapadia SR, Schoenhagen P, Stewart W et al (2010) Imaging for transcatheter valve procedures. Curr Probl Cardiol 35:228–276
32. Laissy JP, Messika-Zeitoun D, Serfaty JM et al (2007) Comprehensive evaluation of preoperative patients with aortic valve stenosis: usefulness of cardiac multidetector computed tomography. Heart 93:1121–1125
33. Ewe SH, Klautz RJ, Schalij MJ et al (2011) Role of computed tomography imaging for transcatheter valvular repair/insertion. Int J Cardiovasc Imaging 27:1179–1193
34. Schoenhagen P, Numburi U, Halliburton SS et al (2010) Three-dimensional imaging in the context of minimally invasive and transcatheter cardiovascular interventions using multidetector computed tomography: from pre-operative planning to intra-operative guidance. Eur Heart J 31:2727–2740
35. Saeed M, Hetts SW, English J et al (2011) MR fluoroscopy in vascular and cardiac interventions (review). Int J Cardiovasc Imaging 28:117–137
36. Siegel RJ, Luo H, Biner S (2011) Transcatheter valve repair/implantation. Int J Cardiovasc Imaging 27:1165–1177
37. Schoenhagen P, Tuzcu EM, Kapadia SR et al (2009) Three-dimensional imaging of the aortic valve and aortic root with computed tomography: new standards in an era of transcatheter valve repair/implantation. Eur Heart J 30:2079–2086
38. Johri AM, Passeri JJ, Picard MH (2010) Three dimensional echocardiography: approaches and clinical utility. Heart 96:390–397
39. Hung J, Lang R, Flachskampf F et al (2007) 3D echocardiography: a review of the current status and future directions. J Am Soc Echocardiogr 20:213–233
40. Handke M, Heinrichs G, Moser U et al (2006) Transesophageal real-time three-dimensional echocardiography methods and initial in vitro and human in vivo studies. J Am Coll Cardiol 48:2070–2076
41. Pothineni KR, Inamdar V, Miller AP et al (2007) Initial experience with live/real time three dimensional transesophageal echocardiography. Echocardiography 24:1099–1104
42. Sugeng L, Shernan SK, Salgo IS et al (2008) Live 3-dimensional transesophageal echocardiography initial experience using the fully-sampled matrix array probe. J Am Coll Cardiol 52:446–449
43. Balzer J, Kelm M, Kühl HP (2009) Real-time three-dimensional transoesophageal echocardiography for guidance of non-coronary interventions in the catheter laboratory. Eur J Echocardiogr 10:341–349
44. Balzer J, Kuhl H, Rassaf T et al (2008) Real-time transesophageal three-dimensional echocardiography for guidance of percutaneous cardiac interventions: first experience. Clin Res Cardiol 97:565–574
45. Scohy TV, Ten Cate FJ, Lecomte PV et al (2008) Usefulness of intraoperative real-time 3D transesophageal echocardiography in cardiac surgery. J Card Surg 23:784–786
46. Sugeng L, Shernan SK, Weinert L et al (2008) Real-time three-dimensional transesophageal echocardiography in valve disease: comparison with surgical findings and evaluation of prosthetic valves. J Am Soc Echocardiogr 21:1347–1354
47. Grewal J, Mankad S, Freeman WK et al (2009) Real-time three-dimensional transesophageal echocardiography in the intraoperative assessment of mitral valve disease. J Am Soc Echocardiogr 22:34–41
48. Iwakura K, Ito H, Kawano S et al (2006) Comparison of orifice area by transthoracic three-dimensional Doppler echocardiography versus proximal isovelocity surface area (PISA) method for assessment of mitral regurgitation. Am J Cardiol 97:1630–1637
49. Sharma R, Mann J, Drummond L et al (2007) The evaluation of real-time 3-dimensional transthoracic echocardiography for the preoperative functional assessment of patients with mitral valve prolapse: a comparison with 2-dimensional transesophageal echocardiography. J Am Soc Echocardiogr 20:934–940
50. Tommasini G, Camerini A, Gatti A et al (1998) Panoramic coronary angiography. J Am Coll Cardiol 31:871–877

51. Schwartz JG, Neubauer AM, Fagan TE et al (2011) Potential role of three-dimensional rotational angiography and C-arm CT for valvular repair and implantation. Int J Cardiovasc Imaging 27:543–546
52. Garcia JA, Chen SY, Messenger JC et al (2007) Initial clinical experience of selective coronary angiography using one prolonged injection and a 180 degrees rotational trajectory. Catheter Cardiovasc Interv 70:190–196
53. Neubauer AM, Garcia JA, Messenger JC et al (2010) Clinical feasibility of a fully automated 3D reconstruction of rotational coronary X-ray angiograms. Circ Cardiovasc Interv 3:71–79
54. Nölker G, Gutleben KJ, Marschang H et al (2008) Three-dimensional left atrial and esophagus reconstruction using cardiac C-arm computed tomography with image integration into fluoroscopic views for ablation of atrial fibrillation: accuracy of a novel modality in comparison with multislice computed tomography. Heart Rhythm 5:1651–1657
55. Biasi L, Ali T, Thompson M (2008) Intra-operative dynaCT in visceral-hybrid repair of an extensive thoracoabdominal aortic aneurysm. Eur J Cardiothorac Surg 34:1251–1252
56. Petersilka M, Bruder H, Krauss B et al (2008) Technical principles of dual source CT. Eur J Radiol 68:362–368
57. Rybicki FJ, Otero HJ, Steigner ML et al (2008) Initial evaluation of coronary images from 320-detector row computed tomography. Int J Cardiovasc Imaging 24:535–546
58. Achenbach S, Marwan M, Ropers D et al (2010) Coronary computed tomography angiography with a consistent dose below 1 mSv using prospectively electrocardiogram-triggered high-pitch spiral acquisition. Eur Heart J 31:340–346
59. Einstein AJ, Henzlova MJ, Rajagopalan S (2007) Estimating risk of cancer associated with radiation exposure from 64-slice computed tomography coronary angiography. JAMA 298:317–323
60. Brenner DJ, Hall EJ (2007) Computed tomography—an increasing source of radiation exposure. N Engl J Med 357:2277–2284
61. Morin RL, Gerber TC, McCollough CH (2003) Radiation dose in computed tomography of the heart. Circulation 107:917–922
62. Halliburton SS, Schoenhagen P (2010) Cardiovascular imaging with computed tomography: responsible steps to balancing diagnostic yield and radiation exposure. JACC Cardiovasc Imaging 3:536–540
63. Hausleiter J, Meyer T, Hermann F et al (2009) Estimated radiation dose associated with cardiac CT angiography. JAMA 301:500–507
64. Hausleiter J, Meyer T, Hadamitzky M et al (2006) Radiation dose estimates from cardiac multislice computed tomography in daily practice: impact of different scanning protocols on effective dose estimates. Circulation 113:1305–1310
65. Bischoff B, Hein F, Meyer T et al (2009) Impact of a reduced tube voltage on CT angiography and radiation dose: results of the PROTECTION I study. JACC Cardiovasc Imaging 2:940–946
66. Herzog BA, Husmann L, Burkhard N et al (2008) Accuracy of low-dose computed tomography coronary angiography using prospective electrocardiogram-triggering: first clinical experience. Eur Heart J 29:3037–3042
67. Husmann L, Valenta I, Gaemperli O et al (2007) Feasibility of low-dose coronary CT angiography: first experience with prospective ECG-gating. Eur Heart J 29:191–197
68. Eggebrecht H, Kuhl H, Kaiser GM (2006) Feasibility of real-time magnetic resonance-guided stent-graft placement in a swine model of descending aortic dissection. Eur Heart J 27:613–620
69. Kuehne T, Yilmaz S, Meinus C (2004) Magnetic resonance imaging-guided transcatheter implantation of a prosthetic valve in aortic valve position: feasibility study in swine. J Am Coll Cardiol 44:2247–2249
70. Kim JH, Kocaturk O, Ozturk C et al (2009) Mitral cerclage annuloplasty, a novel transcatheter treatment for secondary mitral valve regurgitation: initial results in swine. J Am Coll Cardiol 54:638–651

71. Guttman MA, Ozturk C, Raval AN et al (2007) Interventional cardiovascular procedures guided by real-time MR imaging: an interactive interface using multiple slices, adaptive projection modes and live 3D renderings. J Magn Reson Imaging 26:1429–1435
72. Elgort DR, Wong EY, Hillenbrand CM et al (2003) Real-time catheter tracking and adaptive imaging. J Magn Reson Imaging 18:621–626
73. Ratnayaka K, Faranesh AZ, Guttman MA et al (2008) Interventional cardiovascular magnetic resonance: still tantalizing. J Cardiovasc Magn Reson 10:62
74. Ratnayaka K, Raman VK, Faranesh AZ et al (2009) Antegrade percutaneous closure of membranous ventricular septal defect using X-ray fused with MRI (XFM). JACC Cardiovasc Interv 2:224–230
75. Rhode KS, Sermesant M, Brogan D et al (2005) A system for real-time XMR guided cardiovascular intervention. IEEE Trans Med Imaging 24:1428–1440
76. Lam CS, Xanthakis V, Sullivan LM et al (2010) Aortic root remodeling over the adult life course: longitudinal data from the Framingham Heart Study. Circulation 122:884–890
77. Choo SJ, McRae G, Olomon JP et al (1999) Aortic root geometry: pattern of differences between leaflets and sinuses of Valsalva. J Heart Valve Dis 8:407–415
78. Rankin JS, Dalley AF, Crooke PS et al (2008) A 'hemispherical' model of aortic valvar geometry. J Heart Valve Dis 17:179–186
79. Lansac E, Lim HS, Shomura Y et al (2005) Aortic root dynamics are asymmetric. J Heart Valve Dis 14:400–407
80. Lansac E, Lim HS, Shomura Y et al (2002) A four-dimensional study of the aortic root dynamics. Eur J Cardiothorac Surg 22:497–503
81. Kazui T, Izumoto H, Yoshioka K et al (2006) Dynamic morphologic changes in the normal aortic annulus during systole and diastole. J Heart Valve Dis 15:617–621
82. Kazui T, Kin H, Tsuboi J et al (2008) Perioperative dynamic morphological changes of the aortic annulus during aortic root remodeling with aortic annuloplasty at systolic and diastolic phases. J Heart Valve Dis 17:366–370
83. Maselli D, De Paulis R, Scaffa R et al (2007) Sinotubular junction size affects aortic root geometry and aortic valve function in the aortic valve reimplantation procedure: an in vitro study using the Valsalva graft. Ann Thorac Surg 84:1214–1218
84. Kurra V, Kapadia SR, Tuzcu EM et al (2010) Pre-procedural imaging of aortic root orientation and dimensions: comparison between X-ray angiographic planar imaging and 3-dimensional multidetector row computed tomography. JACC Cardiovasc Interv 3:105–513
85. Gurvitch R, Wood DA, Leipsic J et al (2010) Multislice computed tomography for prediction of optimal angiographic deployment projections during transcatheter aortic valve implantation. JACC Cardiovasc Interv 3:1157–1165
86. Tarantini G, Dvir D, Tang GHL (2021) Transcatheter aortic valve implantation in degenerated surgical aortic valves. EuroIntervention 17(9):709–719. https://doi.org/10.4244/EIJ-D-21-00157. PMID: 34665140
87. Tops LF, Wood DA, Delgado V et al (2008) Noninvasive evaluation of the aortic root with multislice computed tomography: implications for transcatheter aortic valve replacement. J Am Coll Cardiol Img 1:321–330
88. Ng ACT, Delgado V, van der Kley F et al (2010) Comparison of aortic root dimensions and geometries before and after transcatheter aortic valve implantation by 2 and 3-dimensional transesophageal echocardiography and multislice computed tomography. Circ Cardiovasc Imaging 3:94–102
89. Akhtar M, Tuzcu EM, Kapadia SR et al (2009) Aortic root morphology in patients undergoing percutaneous aortic valve replacement: evidence of aortic root remodeling. J Thorac Cardiovasc Surg 137:950–956
90. Stolzmann P, Knight J, Desbiolles L et al (2009) Remodelling of the aortic root in severe tricuspid aortic stenosis: implications for transcatheter aortic valve implantation. Eur Radiol 19:1316–1323

91. Schultz CJ, Moelker A, Piazza N et al (2010) Three dimensional evaluation of the aortic annulus using multislice computer tomography: are manufacturer's guidelines for sizing for percutaneous aortic valve replacement helpful? Eur Heart J 31:849–856
92. Doddamani S, Grushko MJ, Makaryus AN et al (2008) Demonstration of left ventricular outflow tract eccentricity by 64-slice multi-detector CT. Int J Cardiovasc Imaging 25:175–181
93. Hutter A, Opitz A, Bleiziffer S et al (2010) Aortic annulus evaluation in transcatheter aortic valve implantation. Catheter Cardiovasc Interv 76:1009–1019
94. Tuzcu EM, Kapadia SR, Schoenhagen P (2010) Multimodality quantitative imaging of aortic root for transcatheter aortic valve implantation: more complex than it appears. J Am Coll Cardiol 55:195–197
95. Messika-Zeitoun D, Serfaty JM, Brochet E et al (2010) Multimodal assessment of the aortic annulus diameter: implications for transcatheter aortic valve implantation. J Am Coll Cardiol 55:186–194
96. Bouzas-Mosquera A, Alvarez-Garcia N, Ortiz-Vazquez E et al (2009) Role of real-time 3-dimensional transesophageal echocardiography in transcatheter aortic valve implantation. Eur J Cardiothorac Surg 35:909
97. Détaint D, Lepage L, Himbert D et al (2009) Determinants of significant paravalvular regurgitation after transcatheter aortic valve: implantation impact of device and annulus discongruence. JACC Cardiovasc Interv 2:821–827
98. Binder RK, Webb JG, Willson AB, Urena M, Hansson NC, Norgaard BL, Pibarot P, Barbanti M, Larose E, Freeman M, Dumont E, Thompson C, Wheeler M, Moss RR, Yang TH, Pasian S, Hague CJ, Nguyen G, Raju R, Toggweiler S, Min JK, Wood DA, Rodés-Cabau J, Leipsic J (2013) The impact of integration of a multidetector computed tomography annulus area sizing algorithm on outcomes of transcatheter aortic valve replacement: a prospective, multicenter, controlled trial. J Am Coll Cardiol 62(5):431–438. https://doi.org/10.1016/j.jacc.2013.04.036. Epub 2013 May 15. PMID: 23684679
99. Tang GHL, Kaneko T, Cavalcante JL (2020) Predicting the feasibility of post-TAVR coronary access and redo TAVR: more unknowns than knowns. JACC Cardiovasc Interv 13(6):736–738. https://doi.org/10.1016/j.jcin.2020.01.222. PMID: 32192694
100. Barbanti M, Costa G, Picci A, Criscione E, Reddavid C, Valvo R, Todaro D, Deste W, Condorelli A, Scalia M, Licciardello A, Politi G, De Luca G, Strazzieri O, Motta S, Garretto V, Veroux P, Giaquinta A, Giuffrida A, Sgroi C, Leon MB, Webb JG, Tamburino C (2020) Coronary cannulation after transcatheter aortic valve replacement: the RE-ACCESS study. JACC Cardiovasc Interv 13(21):2542–2555. https://doi.org/10.1016/j.jcin.2020.07.006. Epub 2020 Oct 14. PMID: 33069648
101. Tang GHL, Zaid S, Fuchs A, Yamabe T, Yazdchi F, Gupta E, Ahmad H, Kofoed KF, Goldberg JB, Undemir C, Kaple RK, Shah PB, Kaneko T, Lansman SL, Khera S, Kovacic JC, Dangas GD, Lerakis S, Sharma SK, Kini A, Adams DH, Khalique OK, Hahn RT, Søndergaard L, George I, Kodali SK, De Backer O, Leon MB, Bapat VN (2020) Alignment of transcatheter aortic-valve neo-commissures (ALIGN TAVR): impact on final valve orientation and coronary artery overlap. JACC Cardiovasc Interv 13(9):1030–1042. https://doi.org/10.1016/j.jcin.2020.02.005. Epub 2020 Mar 16. PMID: 32192985
102. Khan JM, Greenbaum AB, Babaliaros VC, Rogers T, Eng MH, Paone G, Leshnower BG, Reisman M, Satler L, Waksman R, Chen MY, Stine AM, Tian X, Dvir D, Lederman RJ (2019) The BASILICA Trial: prospective multicenter investigation of intentional leaflet laceration to prevent TAVR coronary obstruction. JACC Cardiovasc Interv 12(13):1240–1252. https://doi.org/10.1016/j.jcin.2019.03.035. Epub 2019 Jun 12. PMID: 31202947; PMCID: PMC6669893
103. Latsios G, Gerckens U, Buellesfeld L et al (2010) "Device landing zone" calcification, assessed by MSCT, as a predictive factor for pacemaker implantation after TAVI. Catheter Cardiovasc Interv 76:431–439

104. John D, Buellesfeld L, Yuecel S et al (2010) Correlation of device landing zone calcification and acute procedural success in patients undergoing transcatheter aortic valve implantations with the self-expanding CoreValve prosthesis. J Am Coll Cardiol Intv 3:233–243
105. Zegdi R, Ciobotaru V, Noghin M et al (2008) Is it reasonable to treat all calcified stenotic aortic valves with a valved stent? Results from a human anatomic study in adults. J Am Coll Cardiol 51:579–584
106. Morgan-Hughes GJ, Roobottom CA (2004) Aortic valve calcification on computed tomography predicts the severity of aortic stenosis. Clin Radiol 59:208
107. Willmann JK, Weishaupt D, Lachat M et al (2002) Electrocardiographically gated multidetector row CT for assessment of valvular morphology and calcification in aortic stenosis. Radiology 225:120–128
108. Morgan-Hughes GJ, Owens PE, Roobottom CA et al (2003) Three dimensional volume quantification of aortic valve calcification using multislice computed tomography. Heart 89:1191–1194
109. Cueff C, Serfaty JM, Cimadevilla C et al (2010) Measurement of aortic valve calcification using multislice computed tomography: correlation with haemodynamic severity of aortic stenosis and clinical implication for patients with low ejection fraction. Heart 97:721–726
110. Okura H, Yoshida K, Hozumi T et al (1997) Planimetry and transthoracic two-dimensional echocardiography in noninvasive assessment of aortic valve area in patients with valvular aortic stenosis. J Am Coll Cardiol 30:753–759
111. Poh KK, Levine RA, Solis J et al (2008) Assessing aortic valve area in aortic stenosis by continuity equation: a novel approach using real-time three-dimensional echocardiography. Eur Heart J 29:2526–2535
112. John AS, Dill T, Brandt RR et al (2003) Magnetic resonance to assess the aortic valve area in aortic stenosis: how does it compare to current diagnostic standard. J Am Coll Cardiol 42:519–526
113. Burgstahler C, Kunze M, Loffler C et al (2006) Assessment of left ventricular outflow tract geometry in non-stenotic and stenotic aortic valves by cardiovascular magnetic resonance. J Cardiovasc Magn Reson 8:825–829
114. Del Valle-Fernández R, Jelnin V, Panagopoulos G et al (2010) A method for standardized computed tomography angiography-based measurement of aortic valvar structures. Eur Heart J 31:2170–2178
115. Delgado V, Ng ACT, van de Veire NR et al (2010) Transcatheter aortic valve implantation: role of multi-detector row computed tomography to evaluate prosthesis positioning and deployment in relation to valve function. Eur Heart J 8:113–123
116. Feuchtner GM, Dichtl W, Friedrich GJ et al (2006) Multislice computed tomography for detection of patients with aortic valve stenosis and quantification of severity. J Am Coll Cardiol 47:1410–1417
117. Janosi RA, Kahlert P, Plicht B et al (2009) Guidance of percutaneous transcatheter aortic valve implantation by real-time three-dimensional transesophageal echocardiography—a single-center experience. Minim Invasive Ther Allied Technol 18:142–148
118. Quill JL, Hill AJ, Laske TG et al (2009) Mitral leaflet anatomy revisited. J Thorac Cardiovasc Surg 137:1077–1081
119. Van Mieghem NM, Piazza N, Anderson RH et al (2010) Anatomy of the mitral valvular complex and its implications for transcatheter interventions for mitral regurgitation. J Am Coll Cardiol 56:617–626
120. Maselli D, Guarracino F, Chiaramonti F et al (2006) Percutaneous mitral annuloplasty: an anatomic study of human coronary sinus and its relation with mitral valve annulus and coronary arteries. Circulation 114:377–380
121. Ormiston JA, Shah PM, Tei C et al (1981) Size and motion of the mitral valve annulus in man. I. A two-dimensional echocardiographic method and findings in normal subjects. Circulation 64:113–120

122. Ormiston JA, Shah PM, Tei C et al (1982) Size and motion of the mitral valve annulus in man. II. Abnormalities in mitral valve prolapse. Circulation 65:713–719
123. Pai RG, Tanimoto M, Jintapakorn W et al (1995) Volume-rendered three-dimensional dynamic anatomy of the mitral annulus using a transesophageal echocardiographic technique. J Heart Valve Dis 4:623–627
124. Kaplan SR, Bashein G, Sheehan FH et al (2000) Three dimensional echocardiographic assessment of annular shape changes in the normal and regurgitant mitral valve. Am Heart J 139:378–387
125. Komoda T, Hetzer R, Uyama C et al (1994) Mitral annular function assessed by 3D imaging for mitral valve surgery. J Heart Valve Dis 3:483–490
126. Levine RA, Handschumacher MD, Sanfilippo AJ et al (1989) Three-dimensional echocardiographic reconstruction of the mitral valve, with implications for the diagnosis of mitral valve prolapse. Circulation 80:589–598
127. Faletra F, Grimaldi A, Pasotti E et al (2009) Real-time 3-dimensional transesophageal echocardiography during double percutaneous mitral edge-to-edge procedure. JACC Cardiovasc Imaging 2:1031–1033
128. Swaans MJ, Van den Branden BJ, Van der Heyden JA et al (2009) Three-dimensional transoesophageal echocardiography in a patient undergoing percutaneous mitral valve repair using the edge-to-edge clip technique. Eur J Echocardiogr 10:982–983
129. Daimon M, Shiota T, Gillinov AM et al (2005) Percutaneous mitral valve repair for chronic ischemic mitral regurgitation: a real-time three-dimensional echocardiographic study in an ovine model. Circulation 111:2183–2189
130. Feuchtner GM, Alkadhi H, Karlo C et al (2010) Cardiac CT angiography for the diagnosis of mitral valve prolapse: comparison with echocardiography. Radiology 254:374–383
131. Weir-McCall JR, Blanke P, Naoum C, Delgado V, Bax JJ, Leipsic J (2018) Mitral valve imaging with CT: relationship with transcatheter mitral valve interventions. Radiology 288(3):638–655. https://doi.org/10.1148/radiol.2018172758. Epub 2018 Jul 31. PMID: 30063194
132. Blanke P, Naoum C, Webb J, Dvir D, Hahn RT, Grayburn P, Moss RR, Reisman M, Piazza N, Leipsic J (2015) Multimodality imaging in the context of transcatheter mitral valve replacement: establishing consensus among modalities and disciplines. JACC Cardiovasc Imaging 8(10):1191–1208. https://doi.org/10.1016/j.jcmg.2015.08.004. PMID: 26481845
133. Case BC, Lisko JC, Babaliaros VC, Greenbaum AB, Satler L, Ben-Dor I, Forrestal BJ, Yerasi C, Kamioka N, Rogers T, Waksman R, Lederman RJ, Khan JM (2021) LAMPOON techniques to prevent or manage left ventricular outflow tract obstruction in transcatheter mitral valve replacement. Ann Cardiothorac Surg 10(1):172–179. https://doi.org/10.21037/acs-2020-mv-25. PMID: 33575191; PMCID: PMC7867420
134. Alkadhi H, Desbiolles L, Stolzmann P et al (2009) Mitral annular shape, size, and motion in normals and in patients with cardiomyopathy: evaluation with computed tomography. Investig Radiol 44:218–225
135. Choure AJ, Garcia MJ, Hesse B et al (2006) In vivo analysis of the anatomical relationship of coronary sinus to mitral annulus and left circumflex coronary artery using cardiac multidetector computed tomography: implications for percutaneous coronary sinus mitral annuloplasty. J Am Coll Cardiol 48:1938–1945
136. Gopal A, Shah A, Shareghi S et al (2010) The role of cardiovascular computed tomographic angiography for coronary sinus mitral annuloplasty. J Invasive Cardiol 22:67–73
137. Tops LF, Van de Veire NR, Schuijf JD et al (2007) Noninvasive evaluation of coronary sinus anatomy and its relation to the mitral valve annulus: implications for percutaneous mitral annuloplasty. Circulation 115:1426–1432
138. Kurra V, Schoenhagen P, Roselli EE et al (2009) Prevalence of significant peripheral artery disease in patients evaluated for percutaneous aortic valve insertion: preprocedural assessment with multidetector computed tomography. J Thorac Cardiovasc Surg 137:1258–1264
139. Joshi SB, Mendoza DD, Steinberg DH et al (2009) Ultra-low-dose intra-arterial contrast injection for iliofemoral computed tomographic angiography. JACC Cardiovasc Imaging 2:1404–1411

140. Hahn RT, Nabauer M, Zuber M, Nazif TM, Hausleiter J, Taramasso M, Pozzoli A, George I, Kodali S, Bapat V, Maisano F (2019) Intraprocedural imaging of transcatheter tricuspid valve interventions. JACC Cardiovasc Imaging 12(3):532–553. https://doi.org/10.1016/j.jcmg.2018.07.034. PMID: 30846126
141. Rodés-Cabau J, Hahn RT, Latib A, Laule M, Lauten A, Maisano F, Schofer J, Campelo-Parada F, Puri R, Vahanian A (2016) Transcatheter therapies for treating tricuspid regurgitation. J Am Coll Cardiol 67(15):1829–1845. https://doi.org/10.1016/j.jacc.2016.01.063. PMID: 27081024
142. Dahou A, Levin D, Reisman M, Hahn RT (2019) Anatomy and physiology of the tricuspid valve. JACC Cardiovasc Imaging 12(3):458–468. https://doi.org/10.1016/j.jcmg.2018.07.032. PMID: 30846121
143. Khalique OK, Cavalcante JL, Shah D, Guta AC, Zhan Y, Piazza N, Muraru D (2019) Multimodality imaging of the tricuspid valve and right heart anatomy. JACC Cardiovasc Imaging 12(3):516–531. https://doi.org/10.1016/j.jcmg.2019.01.006. Erratum in: JACC Cardiovasc Imaging. 2019 Dec;12(12):2611–2612. PMID: 30846125
144. van Rosendael PJ, Kamperidis V, Kong WK, van Rosendael AR, van der Kley F, Ajmone Marsan N, Delgado V, Bax JJ (2017) Computed tomography for planning transcatheter tricuspid valve therapy. Eur Heart J 38(9):665–674. https://doi.org/10.1093/eurheartj/ehw499. PMID: 27807057
145. Muraru D, Hahn RT, Soliman OI, Faletra FF, Basso C, Badano LP (2019) 3-dimensional echocardiography in imaging the tricuspid valve. JACC Cardiovasc Imaging 12(3):500–515. https://doi.org/10.1016/j.jcmg.2018.10.035. PMID: 30846124
146. Nickenig G, Weber M, Lurz P, von Bardeleben RS, Sitges M, Sorajja P, Hausleiter J, Denti P, Trochu JN, Näbauer M, Dahou A, Hahn RT (2019) Transcatheter edge-to-edge repair for reduction of tricuspid regurgitation: 6-month outcomes of the TRILUMINATE single-arm study. Lancet 394(10213):2002–2011. https://doi.org/10.1016/S0140-6736(19)32600-5. Epub 2019 Nov 7. Erratum in: Lancet. 2020 Mar 14;395(10227):870. PMID: 31708188
147. Nickenig G, Kowalski M, Hausleiter J et al (2017) Transcatheter treatment of severe tricuspid regurgitation with the edge-to-edge mitraclip technique. Circulation 135:1802–1814
148. Schoenhagen P, Hill A (2009) Transcatheter aortic valve implantation and potential role of 3D imaging. Expert Rev Med Devices 6:411–421
149. Abel DB, Dehdashtian MM, Rodger ST et al (2006) Evolution and future of preclinical testing for endovascular grafts. J Endovasc Ther 13:649–659
150. Zarins CK, Taylor CA (2009) Endovascular device design in the future: transformation from trial and error to computational design. J Endovasc Ther 16(Suppl 1):I12–I21
151. Grbi S, Ionasec R, Vitanovski D et al (2010) Complete valvular heart apparatus model from 4D cardiac CT. Med Image Comput Comput Assist Interv 13:218–226
152. Verhey JF, Nathan NS, Rienhoff O et al (2006) Finite-element-method (FEM) model generation of time-resolved 3D echocardiographic geometry data for mitral-valve volumetry. Biomed Eng Online 3:5–17
153. Conti CA, Votta E, Della Corte A et al (2010) Dynamic finite element analysis of the aortic root from MRI-derived parameters. Med Eng Phys 32:212–221
154. Kaplan AV, Baim DS, Smith JJ et al (2004) Medical device development: from prototype to regulatory approval. Circulation 109:3068–3072
155. Baim DS, Donovan A, Smith JJ et al (2007) Medical device development: managing conflicts of interest encountered by physicians. Catheter Cardiovasc Interv 69:655–664
156. Vassiliades TA Jr, Block PC, Cohn LH et al (2005) The clinical development of percutaneous heart valve technology: a position statement of the Society of Thoracic Surgeons (STS), the American Association for Thoracic Surgery (AATS), and the Society for Cardiovascular Angiography and Interventions (SCAI) Endorsed by the American College of Cardiology Foundation (ACCF) and the American Heart Association (AHA). J Am Coll Cardiol 45:1554–1560

157. Schievano S, Taylor AM, Capelli C et al (2010) First-in-man implantation of a novel percutaneous valve: a new approach to medical device development. EuroIntervention 5:745–750
158. Schievano S, Taylor AM, Capelli C et al (2010) Patient specific finite element analysis results in more accurate prediction of stent fractures: application to percutaneous pulmonary valve implantation. J Biomech 43:687–693
159. Capelli C, Taylor AM, Migliavacca F et al (2010) Patient-specific reconstructed anatomies and computer simulations are fundamental for selecting medical device treatment: application to a new percutaneous pulmonary valve. Philos Transact A Math Phys Eng Sci 368:3027–3038
160. Lurz P, Nordmeyer J, Giardini A et al (2011) Early versus late functional outcome after successful percutaneous pulmonary valve implantation are the acute effects of altered right ventricular loading all we can expect? J Am Coll Cardiol 57:724–731